Desalination and Water Treatment
www.deswater.com
doi: 10.5004/dwt.2021.26524

209 (2021) 197–203
January

Effect of geometrical and operating mixing parameters on copper adsorption on zeolite NaX

Anita Bašić, Sandra Svilović*

Faculty of Chemistry and Technology, University of Split, Ruđera Boškovića 35, 21 000 Split, Croatia, emails: sandra@ktf-split.hr (S. Svilović), abasic@ktf-split.hr (Anita Bašić)

Received 7 April 2020; Accepted 28 August 2020

ABSTRACT

The successful design of the batch reactor and conditions in which heterogeneous reaction is carried out must take into account the effect of hydrodynamic conditions but not only through mixing speed. This design requires knowledge of the effect of various types of impeller, their position, size, and energy input. In this work, kinetic experiments were conducted at different impeller position and N/N_{JS} ratio values (impeller speed/minimum impeller speed for complete suspension). The effect of the turbine impeller off-bottom clearance and N/N_{JS} ratio on power consumption was also studied. The Ritchie model, Mixed surface reaction and diffusion-controlled adsorption kinetic model, and Weber–Morris model were used for assessment of model parameters and the slowest step of the process. The results indicate that the impeller position and N/N_{JS} ratio influence kinetic and power consumption. The greatest difference in power consumption at different impeller positions was obtained for $N/N_{JS} = 1$. Also, it was found that diffusion starts to affect overall kinetic at $N/N_{JS} = 0.7$.

Keywords: Zeolite; Impeller off-bottom clearance; Power consumption; Adsorption; Kinetic

1. Introduction

Zeolites are porous, crystalline alumo-silicates that have transformed the petrochemical and chemical industry due to their application as catalysts and adsorbents. The production of synthetic zeolites has a significant impact on the catalytic process [1]. Catalytic properties of zeolites could be adjusted by "inserting" heavy metals into the zeolite. One of the methods that could be used for the preparation of metal-zeolite catalysts is adsorption. Zeolites could also be used for the removal of metals from contaminated waters by adsorption.

The adsorption process consists of four steps. The first stage is bulk transport, second is film diffusion, then intraparticle diffusion, and finally adsorptive attachment. Bulk transport, that is, transport in the solution usually occurs immediately as zeolite is placed in the adsorbate solution. The last stage, also, occurs very quickly. Hence, both stages are less significant for the design. The second and third steps are often rate-limiting but, using appropriate conditions, this could be prevented [2,3]. The intraparticle diffusion as the rate-limiting step can be avoided by using the appropriate particle size and film diffusion by applying appropriate mixing conditions. The selection of appropriate mixing conditions for adsorption still remains a challenge. In a number of studies, the effect of mixing was completely neglected or just casually mentioned [4,5]. Eventually, the effect of impeller speed was studied [6]. The inadequate design of the batch reactor in terms of optimal settings for mixing and maintaining the system under these settings during the process may cause significant drawbacks regarding product yield and cost [7].

As different impeller rotation speed causes the different states of zeolite suspension and influences adsorption, in this work the effect of mixing parameters, namely the effects of impeller off-bottom clearance and pitch blade turbine

* Corresponding author.

(PBT) impeller speed on copper adsorption on zeolite NaX has been studied. The influence of different impeller positions and N/N_{JS} ratio values on adsorption kinetics was also studied. Using three different kinetic models: Ritchie model, Mixed surface reaction, and diffusion-controlled adsorption kinetic model and Weber–Morris model the slowest step of the process was checked. Linear least square method, nonlinear least square method, and differential equation solver (Mathcad) with Odesolve and Minerr as output functions were used for the calculation of model parameters.

2. Materials and methods

2.1. Materials

Zeolite NaX (Alfa Aesar) was crushed and sieved to obtain a particle diameter 0.063–0.090 mm. Solutions containing copper ions were prepared by dissolving the appropriate weight of $Cu(NO_3)_2{\cdot}3H_2O$ (Kemika) in ultrapure water. The initial concentrations of copper solutions were determined by Perkin Elmer Lambda 25 UV/Vis spectrophotometer at 810 nm (Perkin Elmer, Waltham, MA, USA).

2.2. Experimental procedure

All experiments were carried out in a glass batch reactor with an internal diameter of d_T = 0.14 m (Fig. 1). The height of the solution, H, and internal vessel diameter d_T were equal. The reactor was equipped with four baffles placed at 90° around the vessel periphery. Baffles width, R_v, was equal to 1/10 d_T. The suspension, 2.10 L of the copper solution, and 10.50 g of zeolite, was stirred using the four blades 45° PBT (Fig. 1). Impeller diameter was D = 0.08 m. Firstly, the impeller speed which ensures the state of complete suspension, N_{JS}, was determined by Zwietering's visual method [8] for three impeller off-bottom clearances (C/H = 0.10, 0.33, and 0.50). While finding the critical impeller speed, the base of the reactor was illuminated from all directions by placing a mirror below the reactor bottom and source of light nearby. Impeller speed was gradually increased until all particles of zeolite are in motion, and none remained on the reactor bottom for more than 1 s. The measurements were repeated ten times, and the average value was calculated. Afterwards, kinetic experiments were carried out. These experiments were carried out as a function of PBT impeller speed and position while the temperature (300 K), initial concentration (6.7 mmol/L), and particle diameter were kept constant. At define process times (0.75, 2, 4, 7, 11, 15, 22, 30, 45, 60, 90, 120, 150, 180, 210, 240, 270, 300, 330, and 360 min), the suspension samples were withdrawn from the reactor, centrifuged, and filtrated. The concentration of the copper in the solution was analyzed by UV/Vis spectrophotometer.

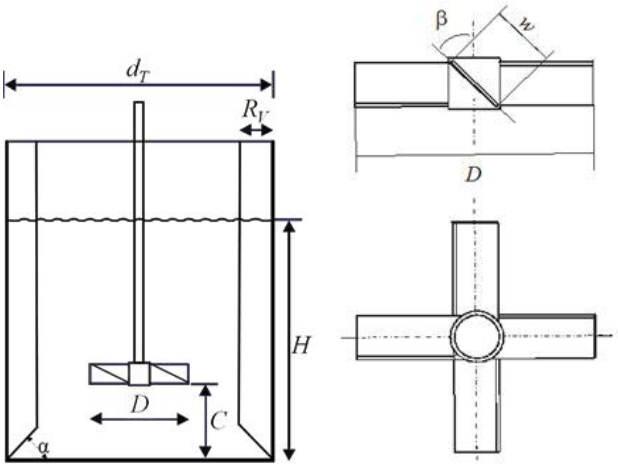

Fig. 1. Design details of baffled batch reactor and pitch blade turbine impeller (D = 0.08 m, w = 0.2 D, and β = 45°).

The amount of copper retained on the zeolite, q_t (mmol/g) was calculated as:

$$q_t = \frac{(c_0 - c_t)V}{m} \tag{1}$$

where c_0 is the initial concentration of copper solution (mmol/L), c_t is the concentration of copper solution at time t (mmol/L), V is the volume of solution (L), and m is the mass of zeolite (g).

For all examined mixing conditions torque was measured by Lightnin LabMaster LB2 and the power consumption, P, was determined by Eq. (2):

$$P = 2\pi N \vartheta \tag{2}$$

where N is the impeller speed (rpm) and ϑ is torque (N cm).

3. Theory/calculation

3.1. Models

Obtained experimental rate data were fitted using Ritchie model, Mixed surface reaction and diffusion-controlled adsorption kinetic model and Weber–Morris model.

The Weber–Morris, diffusion based, model [9] is:

$$q_t = k_d t^{1/2} + I \tag{3}$$

where k_d is the intraparticle diffusion rate constant (mmol/g min$^{1/2}$), t is time (min), and I is the intercept of the vertical axis (mmol/g). If the Weber–Morris plot of q_t vs. $t^{1/2}$ gives a straight line through the origin, I = 0, intraparticle diffusion is considered as the rate-limiting step, while, at I > 0 both film and intraparticle diffusion are considered as rate-limiting steps [10].

The Ritchie rate equation, reaction-based model, is expressed as [11,12]:

$$\frac{d\theta}{dt} = k_r (1-\theta)^n \tag{4}$$

where k_r is the rate constant of the Ritchie model.

After integration, for the boundary conditions θ = θ_0 at $t = t_0$ and θ = θ at $t = t$, and for n = 2 Eq. (4) becomes:

$$q_t = q_e \left(1 - \frac{1}{1 + k_r t}\right) \tag{5}$$

where q_e is the amount of copper ions adsorbed at equilibrium (equilibrium capacity) (mmol/g).

The Mixed surface reaction and diffusion-controlled adsorption kinetic model is expressed as [13]:

$$\frac{dq_t}{dt} = k\left(1+\frac{\tau^{1/2}}{t^{1/2}}\right)\left(c_0 - \frac{c_0 - c_e}{q_e}q_t\right)\left(q_e - q_t\right) \tag{6}$$

After integration:

$$q_t = q_e \frac{e^{\left(at+bt^{1/2}\right)}-1}{u_e e^{\left(at+bt^{1/2}\right)}-1} \tag{7}$$

where $u_e = 1-\frac{c_e}{c_0}$, $a = kc_0\left(u_e-1\right)$, $b = 2kc_0\tau^{1/2}\left(u_e-1\right)$, c_e is the concentration at equilibrium (mmol/L), τ is a parameter that defines the contribution of a diffusion process on the rate of the adsorption (min); if τ > 0 diffusion affects the kinetics.

3.2. Calculations

Model parameters were calculated using linear (Weber–Morris model) or non-linear least square method (Ritchie model and Mixed surface reaction and diffusion-controlled adsorption kinetic model – integrated form). The plan was to solve a differential form of Ritchie and Mixed surface reaction and diffusion-controlled adsorption kinetic model using a differential equation solver and to compare values of calculated parameters. Mathcad (PTC) was used for all calculations.

The goodness of fit of applied kinetic models was analyzed using average absolute relative deviation AARD (%) which is considered to be acceptable up to 5%, and above 10% indicates a poor approximation of the model predicted values [14]:

$$\text{AARD} = \frac{1}{n}\sum_{i=1}^{n}\left[\left|\frac{q_{t_i} - q_{t\_\text{model}_i}}{q_{t_i}}\right|100\right] \tag{8}$$

where q_t is the experimental value of q_t,and $q_{t_}$model is the calculated value of q_t.

The parameters of Ritchie and mixed-surface reaction and diffusion-controlled adsorption kinetic model were calculated from the kinetics Eqs. (5) and (7) using the solve block and Minerr as the output function:
For Ritchie model:

$$\frac{d}{dX}\sum_{i=1}^{n}\left[q_{t_i} - \left(q_e\left(1-\frac{1}{1+k_r t_i}\right)\right)\right]^2 = 0 \tag{9}$$

For mixed surface reaction and diffusion controlled adsorption kinetic model:

$$\frac{d}{dX}\sum_{i=1}^{n}\left[q_{t_i} - \left(\frac{e^{kc_0\left(u_e-1\right)t_i+\left[2kc_0\tau^{1/2}\left(u_e-1\right)\right]t_i^{\frac{1}{2}}}-1}{u_e e^{kc_0\left(u_e-1\right)t_i+\left[2kc_0\tau^{1/2}\left(u_e-1\right)\right]t_i^{\frac{1}{2}}}-1}\right)\right]^2 = 0 \tag{10}$$

where X is a model parameter (k_r and q_e for Ritchie model and u_e, k, t, and q_e for Mixed surface reaction and diffusion-controlled adsorption kinetic model). The number of equations is equal to the number of parameters.

For solving differential forms of Ritchie and mixed-surface reaction and diffusion-controlled adsorption kinetic model solve blocks were used with Odesolve and Minerr as output functions.

4. Results and discussion

In order to obtain fast adsorption on the particle–solution contact area, it is needed to achieve a maximum surface area of particles and minimum film thickness around them. This is the reason why is so important to optimize hydrodynamic conditions in the reactor, to avoid an accumulation of zeolite particles in any part of the reactor, and to enable their free movement through the entire volume of solution. This can usually be obtained for just-suspended conditions, that is, at critical impeller speed for just off-bottom suspension, N_{JS}. Consequently, the first goal was to find N_{JS} for three positions of the impeller. The obtained values at C/H = 0.10, 0.33, and 0.50 are 143, 230, and 284 rpm, respectively. Since all data are obtained for the same mass of zeolite and the same range of particle sizes, these results can be attributed to the flow pattern generated by the different impeller position. PBT generates mainly an axial flow, but with a noticeable radial component and therefore is considered mixed flow impeller. At higher C/H, due to the impeller discharge, the reverse loop that is created in the area under the impeller is more pronounced. This reverse loop causes a stagnant zone, a decrement of turbulence in the reactor, and the just-suspended conditions are achieved at a higher impeller speed [15].

Since energy savings may be more important than some other parameter, which benefits from higher impeller speed, some processes operate at the impeller speed that is lower than N_{JS} [7]. For this reason, kinetic experiments were obtained not only for N_{JS} (N/N_{JS} = 1) but for N/N_{JS} equal to 0.8, 0.7, 0.6, 0.5, and 0.4 as well. At the same time, the contribution of diffusion on overall kinetics for various hydrodynamic conditions was found. The influence of impeller position and speed on kinetics were studied at three different positions and for every position at six impeller speed. The results of this study are shown in Fig. 2 and the parameters calculated from these data in Table 1. For all experiments, kinetic data in Fig. 2 are presented for the entire span of the experiment and the first 15 min in order to see the difference or concurrence in the initial stage of adsorption.

The presented data show that adsorption capacity is almost equal for N/N_{JS} in the range from 1 to 0.6 but with a less pronounced agreement with higher off-bottom clearance. For further divergence from the N_{JS}, a decrease in capacity is noticeable. This is the result of an accumulation of zeolite particles on the bottom of the reactor and unavailability of the entire zeolite surface.

The difference or concurrence of the time required for achieving the equilibrium at N/N_{JS} = 1 and all other N/N_{JS} ratio depends, not only on this ratio but on impeller position as well. The impeller speed has the least impact for lowest impeller off-bottom clearance and at this position,

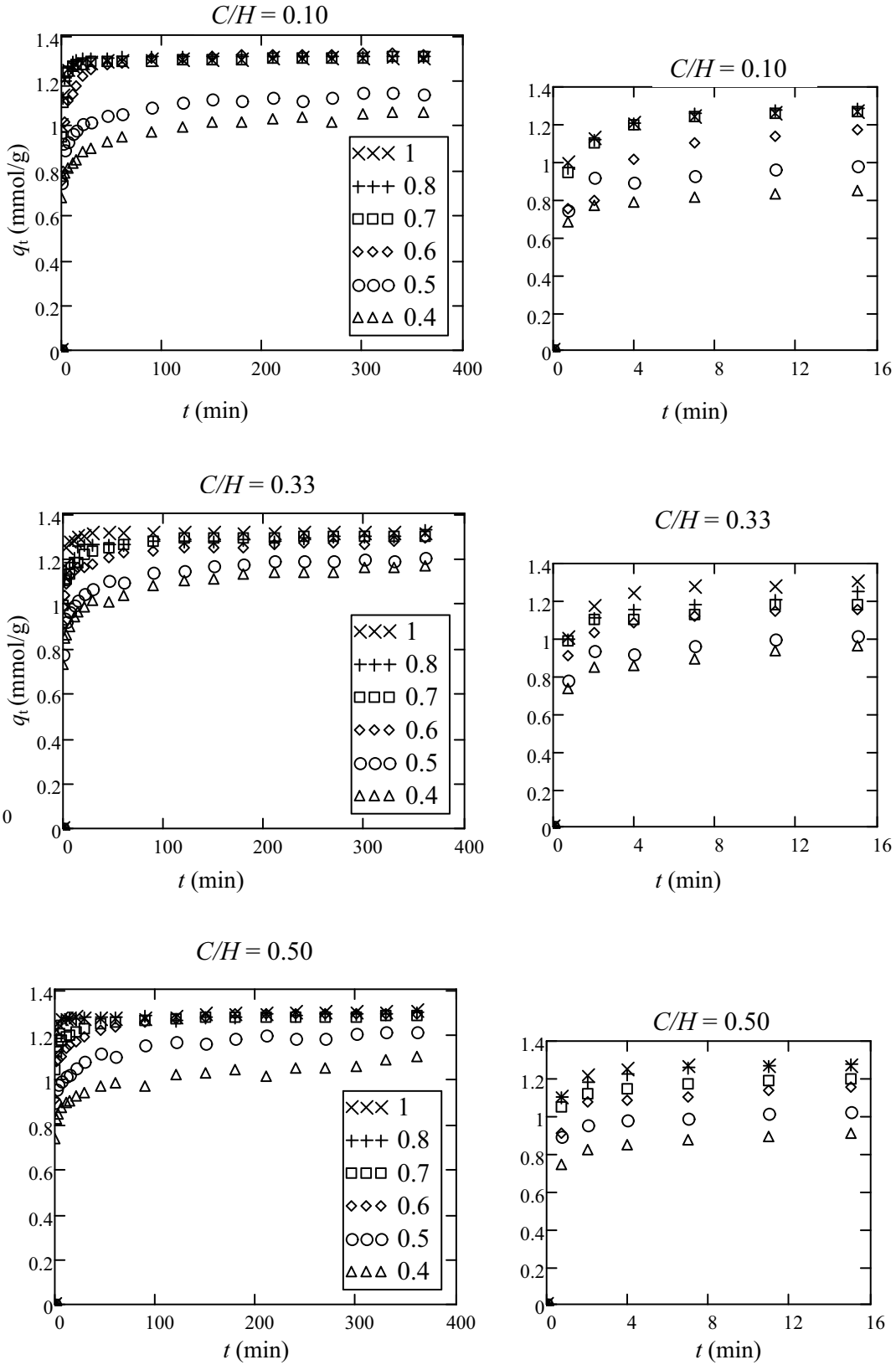

Fig. 2. Experimental kinetics data at different off-bottom clearance and N/N_{JS} ratio (left – entire span of experiment, right – first 15 min).

Table 1
Calculated parameters of kinetic models used for various impeller speed and position

Model	Parameter	N_{JS}	0.8 N_{JS}	0.7 N_{JS}	0.6 N_{JS}	0.5 N_{JS}	0.4 N_{JS}
D = 8.0 cm (D/d_T = 0.57) PBT C/H = 0.10							
Experimental data	$q_{e,exp}$ (mmol/g)	1.305	1.306	1.305	1.303	1.148	1.060
Ritchie model (non-linear least square method)	k_r (g/mmol min)	4.151	3.663	3.421	1. 117	2.270	1.922
	q_e (mmol/g)	1.293	1.305	1.294	1.296	1.082	0.977
	AARD (%)	0.565	0.400	0.479	3.429	4.629	6.248
Ritchie model (Odesolver)	k_r (g/mmol min)	4.194	3.695	3.447	1.117	2.276	1.924
	q_e (mmol/g)	1.293	1.305	1.294	1.296	1.082	0.977
	AARD (%)	0.566	0.393	0.476	3.429	4.626	4.249
Weber–Morris model	k_d (mmol/g min$^{1/2}$)	0.021	0.021	0.021	0.032	0.025	0.026
	I (mmol/g)	1.016	1.025	1.005	0.864	0.763	0.660
	AARD (%)	7.078	7.541	7.495	9.961	7.199	6.535
Mixed surface reaction and diffusion controlled adsorption kinetic model (non-linear least square method)	$u_{e,exp}$ (–)	0.975	0.975	0.975	0.972	0.857	0.803
	q_e (mmol/g)	1.294	1.308	1.298	1.322	1.126	1.029
	k (L/mmol min)	0.515	0.416	0.347	0.037	0.017	0.013
	τ (min)	0.012	0.023	0.058	4.156	71.994	88.020
	u_e (–)	0.999	0.999	0.999	0.982	0.999	0.999
	AARD (%)	0.487	0.400	0.375	1.236	2.514	3.683
D = 8.0 cm (D/d_T = 0.57) PBT C/H = 0.33							
Experimental data	$q_{e,exp}$ (mmol/g)	1.310	1.301	1.300	1.291	1.204	1.164
Ritchie model	k_r (g/mmol min)	4.248	4.006	3.749	2.953	2.071	1.790
	q_e (mmol/g)	1.315	1.277	1.265	1.233	1.136	1.083
	AARD (%)	0.244	1.551	2.820	2.913	5.079	5.857
Weber–Morris model	k_d (mmol/g min$^{1/2}$)	0.020	0.022	0.024	0.025	0.028	0.028
	I (mmol/g)	1.043	0.978	0.956	0.911	0.789	0.731
	AARD (%)	7.348	6.764	6.868	6.955	7.104	6.875
Mixed surface reaction and diffusion controlled adsorption kinetic model	$u_{e,exp}$ (–)	0.978	0.970	0.970	0.962	0.928	0.888
	q_e (mmol/g)	1.316	1.268	1.287	1.262	1.183	1.136
	k (L/mmol min)	0.572	0.550	0.083	0.048	0.021	0.016
	τ (min)	2×10^{-3}	0.011	6.296	14.405	42.233	48.712
	u_e (–)	0.999	0.999	0.999	0.999	0.999	0.999
	AARD (%)	0.245	1.723	1.636	1.293	2.820	3.284
D = 8.0 cm (D/d_T = 0.57) PBT C/H = 0.50							
Experimental data	$q_{e,exp}$ (mmol/g)	1.305	1.299	1.283	1.288	1.211	1.101
Ritchie model	k_r (g/mmol min)	8.092	7.512	5.322	2.911	3.256	2.571
	q_e (mmol/g)	1.287	1.282	1.254	1.248	1.138	1.005
	AARD (%)	0.627	0.583	2.215	3.436	4.988	5.061
Weber–Morris model	k_d (mmol/g min$^{1/2}$)	0.018	0.018	0.022	0.026	0.026	0.024
	I (mmol/g)	1.048	1.042	0.979	0.917	0.824	0.710
	AARD (%)	6.430	6.558	6.772	7.132	6.611	6.545
Mixed surface reaction and diffusion controlled adsorption kinetic model	$u_{e,exp}$ (–)	0.975	0.970	0.958	0.960	0.932	0.813
	q_e (mmol/g)	1.285	1.283	1.272	1.278	1.172	1.042
	k (L/mmol min)	0.795	0.696	0.454	0.050	0.039	0.025
	τ (min)	0.038	0.063	0.137	12.934	23.711	39.270
	u_e (–)	0.973	0.992	0.999	0.999	0.998	0.999
	AARD (%)	0.731	0.567	1.796	1.973	3.177	3.130

for impeller speed equal to N/N_{JS} = 1, 0.8, and 0.7, equilibrium is achieved around 8–10 min. For these experiments τ, from Mixed surface reaction and diffusion-controlled adsorption kinetic model, is under 0.01 meaning that diffusion is negligible. This is confirmed by the agreement of other models used with experimental data. Ritchie, reaction based, model shows the good agreement, and Weber–Morris, diffusion based, model the worst agreement. For the highest off-bottom clearance, the concurrence between experimental kinetic data exists for the two highest N/N_{JS} ratio, as for standard off-bottom clearance, but in these experiments only for the first few sampling points. For these data τ is, also, under 0.01 and agreement between models used and experimental data is the same as above.

For other experiments, the effect of diffusion could not be neglected. Agreement with Ritchie model, and q_e calculated by Ritchie model with q_e experimental, decrease with decreasing N/N_{JS} ratio for all positions. The value of its rate constant also decreases with decreasing N/N_{JS} ratio for all positions, indicating a decrease in rate. For these data Mixed surface reaction and diffusion-controlled adsorption kinetic model show the best agreement and the values of τ is in the range from 4.156 to 88.020 min depending on N/N_{JS} ratio and *C/H.* As expected, the highest values of τ are obtained for the lowest N/N_{JS} ratio. Agreement between q_e calculated by this model and q_e obtained experimentally is fitting no matter what the slowest process is. But the u_e experimental did not agree with the calculated ones very well. This model, for our data, predicts the highest possible value of u_e that corresponds with the theoretical one.

Calculation of parameters was successfully completed for both linear and non-linear least square method while for differential equation solver only the calculations for Ritchie model were successful. Mixed surface reaction and diffusion controlled adsorption kinetic model could not be solved this way.

As can be seen from Table 1, parameters of Ritchie model obtained by non-linear least square method and differential equation solver are practically the same. For this reason, the parameters obtained by differential equation solver are presented only for *C/H* = 0.10.

The last step of this study was the calculation of power consumption not only for N_{JS} but for all impeller speed used. Higher velocity should yield higher power consumption, so the economical point of view should be considered. According to Eq. (2), power consumption is proportional to the impeller speed. Lower impeller speed resulted in lower power consumption. As can be seen from Fig. 3, the lowest

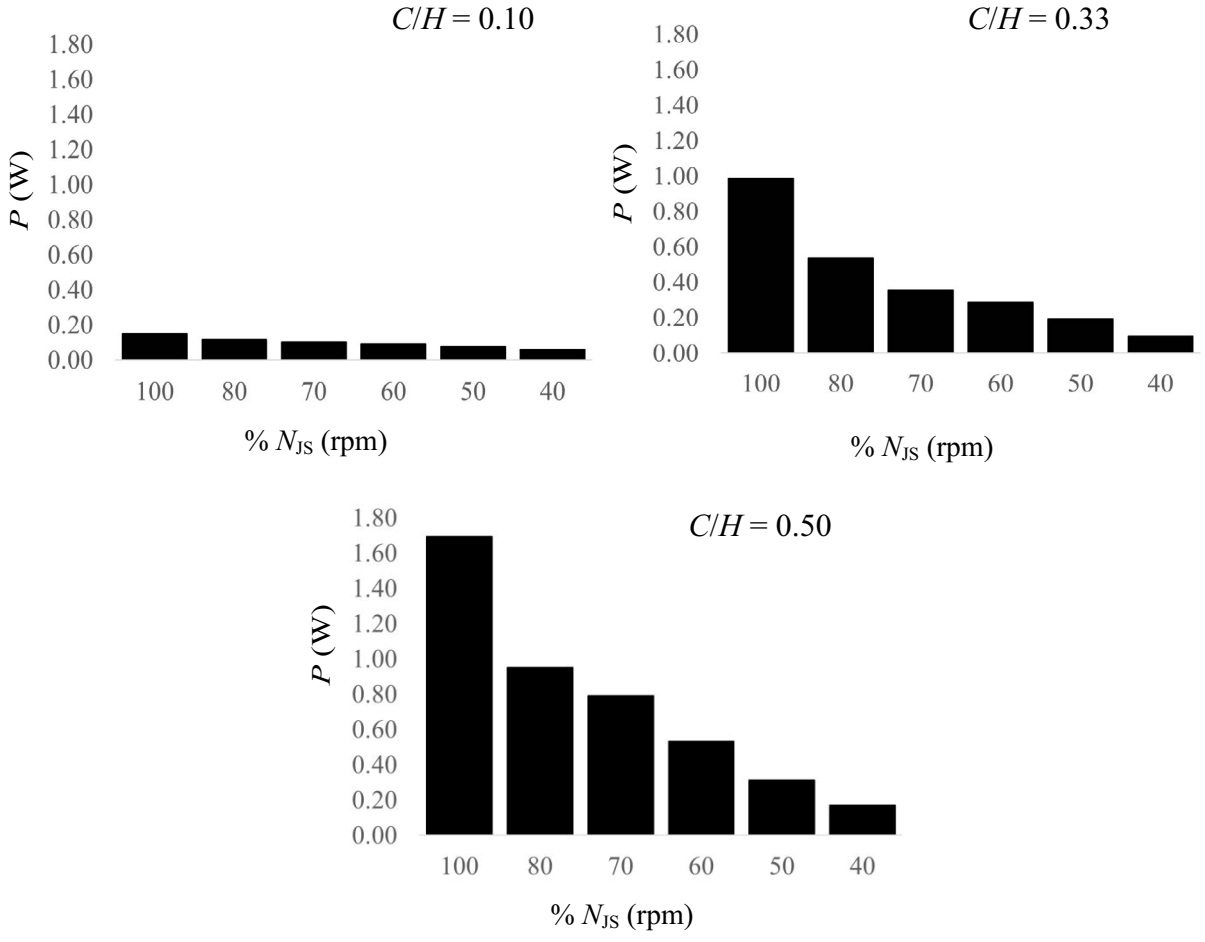

Fig. 3. Effect of impeller speed and off-bottom clearance on power consumption.

values of P were obtained for C/H = 0.10 and the highest for C/H = 0.50. The greatest difference in power consumption at different impeller positions was obtained for N/N_{JS} = 1 (power consumption at C/H = 0.10 was only 8.8% of power consumption at C/H = 0.50). This difference decreased with increasing the divergence form N_{JS} and for N/N_{JS} = 0.4 power consumption at C/H = 0.10 was 34.7% of power consumption at C/H = 0.50).

5. Conclusion

Based on the findings of the effect of PBT impeller position and N/N_{JS} ratio on copper adsorption kinetic and power consumption several conclusions can be drawn. Regarding achieving the complete suspension it was noticed that the impeller speed for just off-bottom suspension increases with off-bottom clearance. The corresponding dependence was found for power consumption. The effect of the N/N_{JS} ratio on power consumption is the opposite; it decreases with the decrease of N/N_{JS} ratio. The experimental kinetic data can be fitted to all models used. The best fit depends on the N/N_{JS} ratio and off-bottom clearance. For lowest off-bottom clearance, the effect of diffusion is evident for N/N_{JS} = 0.6 and lower values of N/N_{JS} ratio. For 0.33 and 0.50 off-bottom clearance diffusion starts to effect overall kinetic even at N/N_{JS} = 0.7. If the effect of the slowest process and power consumption are taken into account, it is evident that copper adsorption on NaX, at certain conditions, is kinetic controlled and can be economically carried out at partial suspension. With all stated in mind, to carry out the examined process under optimal economic and kinetic conditions, the C/H = *0.10* and N/N_{JS} = 0.7 should be used.

Symbols

AARD — Average absolute relative deviation, %
C — Impeller clearance from bottom, m
c_0 — Initial concentration of metal in solutions, mmol/L
c_e — Equilibrium concentration of metal in solutions, mmol/L
c_t — Concentration of metal in solution at time t, mmol/L
D — Impeller diameter, m
d_T — Reactor internal diameter, m
H — Solution height, m
I — Intercept of the vertical axis, mmol/g
k — Constant of Mixed surface reaction and diffusion-controlled adsorption kinetic model, L/mmol min
k_d — Intraparticle diffusion rate constant, mmol/g min$^{1/2}$
k_r — Rate constant of the Ritchie model, g/mmol min
m — Weight of zeolite NaX, g
N — Impeller speed, rpm
N_{JS} — Impeller speed which ensures the state of complete suspension (just suspended impeller speed), rpm
P — Power consumption, W
q_e — Amount of copper sorbed at equilibrium per gram of zeolite, mmol/g
q_t — Amount of copper sorbed at time t per gram of zeolite, mmol/g
R_v — Baffles width, m
T — Temperature, K
t — Time, min
u_e — Relative equilibrium uptake, –
V — Volume, L
w — Impeller width, m
β — Impeller blade incline, °
ϑ — Torque, N cm
τ — Parameter that defines the contribution of a diffusion process, min

References

[1] B. Yilmaz, U. Müller, Catalytic applications of zeolites in chemical industry, Top. Catal., 52 (2009) 888–895.
[2] W.J. Weber, Evolution of a technology, J. Environ Eng., 110 (1984) 899–917.
[3] H.N. Tran, S.-J. You, A. Hosseini-Bandegharaei, H.-P. Chao, Mistakes and inconsistencies regarding adsorption of contaminants from aqueous solutions: a critical review, Water Res., 120 (2017) 88–116.
[4] X. Liu, Z.-Q. Chen, B. Han, C.-L. Su, Q. Han, W.-Z. Chen, Biosorption of copper ions from aqueous solutions using rape straw powders: optimization, equilibrium and kinetic studies, Ecotoxicol. Environ. Saf., 150 (2018) 251–259.
[5] W. Cao, Z. Wang, H. Ao, B. Yuan, Removal of Cr(VI) by corn stalk based anion exchanger the extent and rate of Cr(VI) reduction as side reaction, Colloid Surf. A, 539 (2018) 424–432.
[6] V.J. Inglezakis, N.A. Diamandis, M.D. Loizidou, H.P Grigoropoulou, Effect of pore clogging on kinetics of lead uptake by clinoptilolite, J. Colloid Interface Sci., 215 (1999) 54–57.
[7] R. Jafari, P.A. Tanguy, J. Chaouki, Characterization of minimum impeller speed for suspension of solids in liquid at high solid concentration using gamma-ray densitometry, Int. J. Chem. Eng., 2012 (2012) 1–15, doi: 10.1155/2012/945314.
[8] T.N. Zwietering, Suspending of solid particles in liquid by agitators, Chem. Eng. Sci., 8 (1958) 244–253.
[9] W.J. Weber, J.C. Morris, Kinetics of adsorption on carbon from solution, J. Sanitary Eng. Div., 2 (1963) 31–60.
[10] S. Svilović, D. Rušić, R. Stipišić, Modeling batch kinetics of copper ions sorption using synthetic zeolite NaX, J. Hazard. Mater., 170 (2009) 941–947.
[11] G. Ritchie, Alternative to Elovich equation for the kinetics of adsorption of gasses on solids, J. Chem. Soc., Faraday Trans. 1 F, 73 (1977) 1650–1653.
[12] W. Cheung, J.F. Porter, G. McKay, Sorption kinetic analysis for the removal of cadmium ions from effluents using bone char, Water Res., 35 (2001) 605–612.
[13] M. Haerifar, S. Azizian, Mixed surface reaction and diffusion – controlled kinetic model for adsorption at the solid/solution interface, J. Phys. Chem. C, 117 (2013) 8310–8317.
[14] J. Vladić, Z. Zeković, S. Jokić, S. Svilović, S. Kovačević, S. Vidović, Winter savory: supercritical carbon dioxide extraction and mathematical modeling of extraction process, J. Supercrit. Fluids, 117 (2016) 89–97.
[15] A. Kaćunić, M. Akrap, N. Kuzmanić, Effect of impeller type and position in batch cooling crystallizer on the growth of borax decahydrate crystals, Chem. Eng. Res. Des., 91 (2013) 274–285.